

This is the accepted manuscript made available via CHORUS. The article has been published as:

## Memory erasure using time-multiplexed potentials

Saurav Talukdar, Shreyas Bhaban, and Murti V. Salapaka

Phys. Rev. E **95**, 062121 — Published 19 June 2017

DOI: [10.1103/PhysRevE.95.062121](https://doi.org/10.1103/PhysRevE.95.062121)

# Memory Erasure using Time Multiplexed Potentials

Saurav Talukdar, Shreyas Bhaban and Murti V. Salapaka  
*University of Minnesota, Minneapolis, USA.*

(Dated: May 25, 2017)

We study the thermodynamics of a Brownian particle under the influence of a time multiplexed harmonic potential of finite width. The memory storage mechanism and the erasure protocol based on time multiplexed potentials are utilized to experimentally realize erasure with work done close to the Landauer's bound. We quantify the work done on the system with respect to the duty-ratio of time multiplexing, which also provides a handle to approach reversible erasures. A Langevin dynamics based simulation model is developed for the proposed memory bit and the erasure protocol, which guides the experimental realization. The study also provides insights into transport at the micro scale.

**PACS numbers:** 05.40.-a, 05.70.Ln

Landauer's principle, pioneered by Rolf Landauer in 1961, provides a critical link between information theory and thermodynamics of physical systems [1]. It states that there is no process where the work done to erase one bit of information is less than  $k_b T \ln 2$  (Landauer's bound), when the prior probability of the bit being in any of the two states is equal [2]. Here,  $k_b$  is the Boltzmann constant and  $T$  is the temperature of the heat bath.

Numerous analyses have corroborated Landauer's bound through different approaches [3–7]. The experimental study of Landauer's bound has only recently become viable, enabled by tools that provide access to processes with energetics in the scale of  $k_b T$ . A first such study in [8] examined Landauer's bound, by employing optical traps to realize a single bit memory. Bechhoefer et.al. [9, 10] used an anti-Brownian electrokinetic feedback trap and Hong et.al. [11] used nano magnetic memory bits to study Landauer's bound.

In this article, we study the stochastic energetics of transport realized by time multiplexing a harmonic potential of finite width, to realize a bi-stable potential. Here a single laser in an optical tweezer setup, is multiplexed between two locations with varying dwell times to create potentials (symmetric as well as asymmetric bi-stable potentials), that effectuate the erasure process. Furthermore, experimental variables to realize reversible erasure are identified and utilized for approaching the Landauer's bound. Langevin dynamics based simulations of a Brownian particle under the influence of a time multiplexed laser is developed and is shown to obey quantitative trends observed in experiments. We use our method of shaping the potential, by changing the dwell time of multiplexing of the laser, to erase one bit of information. The ease of implementation and the high-resolution accounting of energetics are advantages of the method reported. We resort to Sekimoto's stochastic energetics [12–15] framework to quantify the work done on the system for the erasure process. The underlying principles developed in this article are applicable toward the study of transport achieved by time multiplexing of a single potential, where realizations based on optical traps can be considered a particular instantiation of the general un-

derpinnings of the framework presented.

## I. Model for a One-Bit Memory

We use the abstraction of a Brownian particle in a double well potential to model a one-bit memory. The memory is designated the state 'zero' if the particle is in the left well, and the state 'one' if it is in the right well. Experimentally, we realize a Brownian particle in a harmonic potential, albeit of finite width, by using a custom built optical tweezer setup to trap (near the focus of the objective lens) a polystyrene bead ( $1\mu\text{m}$  in diameter) while suspended in deionized water. The bead represents the thermodynamic system of interest with the surrounding medium acting as a heat bath.

**Bead in a Laser Trap:** A laser passing through a high numerical aperture objective lens and incident on a bead in a solution traps the bead. Here, the bead experiences a harmonic potential with the equilibrium point (trap center) located near the focus of the lens. For small displacements away from the centre of the trap, the bead experiences a restoring force directed towards the trap center [16, 17]; the trap behaves like a Hookean spring with the restoring force being  $k\Delta x$ , where  $k$  is the stiffness of the trap and  $\Delta x$  the distance between the bead center and the trap center. The position of the bead (denoted by  $x$ ) is measured using a photo diode for a duration much larger than the time constant of the dynamics of the bead in the laser trap ( $\sim 1\text{ms}$ ). The equilibrium probability distribution,  $P(x)$ , of the position of the bead, is then obtained by binning the measured position data. The potential energy landscape,  $U(x)$ , of the bead in thermal equilibrium with the trap is obtained using the relation,  $U(x) = -\ln(\frac{P(x)}{C})$ , where  $C$  is the normalization constant. In Fig. 1, the potential energy landscape experienced by an optical bead in a laser trap is shown (red and black curves), which is constant outside a distance  $w$  from the minimum of the potential and harmonic within the distance  $w$  from the equilibrium point.

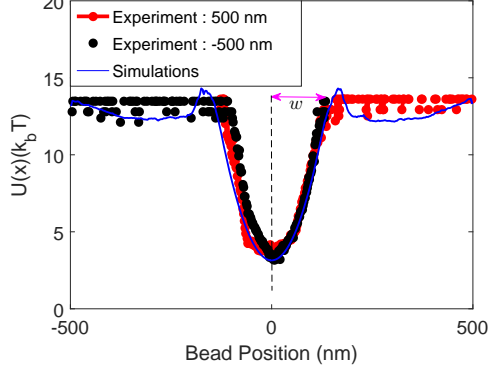


FIG. 1. Potential energy landscape of a bead in a laser trap. The experiments are performed with the bead initially at 500 nm (red curve) and -500 nm (black curve). The position of the bead is measured for 50 seconds. The potential  $U(x)$  is mostly flat after a certain distance  $w$  from the stable equilibrium point. In the Monte Carlo simulations, the bead is initialized randomly between 500 nm and -500 nm. The position trajectory of the bead obtained from 100 Monte Carlo simulations is collected to determine  $U(x)$  from simulations (blue curve).

The potential energy  $U(x)$  is modeled by,

$$U(x) = \begin{cases} \frac{1}{2}kx^2 + U_r, & \text{if } |x| \leq w \\ \frac{1}{2}kw^2 + U_r, & \text{if } |x| > w, \end{cases} \quad (1)$$

which is harmonic up till a distance  $w$  (determined empirically from Fig. 1) from the stable equilibrium point. The stiffness  $k$  of the optical trap is determined experimentally by applying the Equipartition Theorem, that yields  $k = k_b T / \langle x^2 \rangle$  [18]. The dynamics of the bead in a trap is modeled by the over-damped Langevin equation [15],

$$-\gamma \frac{dx}{dt} + \xi(t) - \frac{\partial U(x)}{\partial x} = 0, \quad (2)$$

where,  $\gamma$  is the coefficient of viscosity (determined experimentally by step response method [17]),  $U(x)$  is the potential realized by the trap and  $\xi(t)$  is a zero mean uncorrelated Gaussian noise force. Here,  $\langle \xi(t) \rangle = 0$ ,  $\langle \xi(t), \xi(t') \rangle = 2D\delta(t - t')$  with the diffusion coefficient  $D = \gamma k_b T$ . The potential  $U(x)$  described by (1) is used in conjunction with (2) to obtain 100 realizations (of 20 seconds each) of the bead trajectories. These realizations are, in turn, used to reconstruct the potential felt by the bead by binning the position trajectories. A close match with experimental results is seen, as shown in Fig. 1.

**Double Well Potential Model of Memory:** A double well potential with two locally stable equilibrium points located at  $L$  and  $-L$  is created by alternately focusing the trapping laser between the two locations by time-multiplexing using an Acousto Optical Deflector. The laser is multiplexed at least 100 times faster than the time constant of the dynamics of the bead. The trapping laser

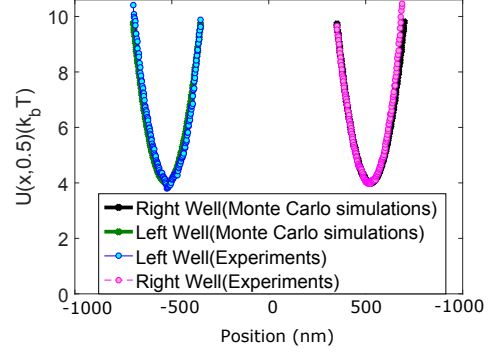


FIG. 2. Double well potential for  $L = 550$  nm obtained using Monte-Carlo simulations and experiments.

multiplexed at the two locations is the external agent coupled to the thermodynamic system of interest formed by the bead. We define duty-ratio  $d$  as the fraction of the total time-period the laser spends at the location  $-L$ . The nature of the effective potential experienced by the Brownian particle can be manipulated by adjusting the duty-ratio. The potential energy landscape,  $U(x, d)$ , experienced by the bead for a duty-ratio  $d$ , is determined by the relationship  $P_d(x) = C e^{-U(x, d)/k_b T}$ , where  $P_d(x)$  is determined by binning the measured position of the bead. Maintaining a duty-ratio of 0.5 results in near identical parabolic potential wells at  $L$  and  $-L$  as shown in Fig. 2, while a duty-ratio greater than 0.5 leads to asymmetric double well potentials as shown in Fig. 3.

The bead dynamics under the influence of time multiplexed potential is modeled by the following Langevin equation,

$$-\gamma \frac{dx}{dt} + \xi(t) - \frac{\partial U(x, d)}{\partial x} = 0, \quad (3)$$

where, the model for the potential  $U(x, d)$  used in (3) incorporates the experimental observation that, for the duration when the laser remains focused at the location  $L$  or  $-L$ , the bead experiences a harmonic potential up till a distance  $w$  from the trap focus. However, beyond the distance  $w$  from the locally stable equilibrium points  $L$  or  $-L$ , the bead undergoes a random walk [19]. Based on these observations, the potential  $U(x, d)$  is modeled by,

$$U(x, d) = \begin{cases} \frac{1}{2}k(x - L)^2 + U_r, & \text{if } |x - L| \leq w, r(t) = 1, \\ \frac{1}{2}k(x + L)^2 + U_r, & \text{if } |x + L| \leq w, r(t) = 0, \\ \frac{1}{2}kw^2 + U_r, & \text{otherwise,} \end{cases} \quad (4)$$

where,  $r(t)$  denotes the binary variable representing the presence/absence status of the laser at  $L$ . If the laser is focused at  $L$ , then  $r(t) = 1$ , otherwise  $r(t) = 0$ . The stiffness of the laser trap,  $k$ , and the width of the corresponding parabolic potential,  $w$ , are determined by characterization of the finite width harmonic potential obtained due to a single trap, as described earlier in (1).

The laser is multiplexed between the two locations at a significantly faster rate ( $\sim 10\mu s$ ) than the time constant of the bead dynamics ( $\sim 1ms$ ), which supports the model in (4). Monte Carlo simulations performed using (3) and the subsequent potential  $U(x, d)$  reconstructed from bead position data, (using the canonical distribution) yield potentials that match closely with experimental observations as seen in Fig. 2. We remark that in the Monte Carlo simulations as well as in experiments, the stiffness of each of the wells formed at  $L$  and  $-L$  when the duty-ratio is 0.5 is close to  $\frac{k}{2}$ , which is half the stiffness of the single trap. In summary, the model parameters ( $k$  and  $w$ ) determined for a single trap is used in the Monte Carlo simulations of the bead in a double well potential realized by time multiplexing of the trapping laser. A close match between simulation and experimental results is observed as shown in Fig. 2. Using the Brownian particle in a double well potential model of a single bit memory, we next present an erasure protocol based on multiplexing of potentials.

## II. Erasure Process

Erasure is a logically irreversible operation [20], where irrespective of the initial state of the memory, the final state is zero (also known as ‘reset-to-zero’ operation). A bead in a double well potential is used to model a single bit memory. No prior information on the state of the memory is assumed initially; thus, it is equally likely that the memory assumes the state zero or one. However, at the end of erasure process the memory state is *zero* (the bead must be in the left well). Thus, there is no change in average energy of the bead in an erasure process (as the depth of both wells is the same) while the decrease in entropy associated with erasure is  $k_b \ln 2$ ; thereby requiring at least  $k_b T \ln 2$  amount of work to be done on the system [2]. We note that the Landauer’s bound is applicable to the average work done on the system over many realizations of the bead trajectory, but, it is possible to obtain individual erasure realizations with the work done on the system less than  $k_b T \ln 2$ . Indeed we demonstrate later that for a fraction of trajectories, the work done on the bead is lower than  $k_b T \ln 2$  (see Fig. 6).

The Landauer’s bound of  $k_b T \ln 2$  holds if the erasure process is always successful. It can be shown that for imperfect erasure schemes with the probability of successful erasure being  $p$ , at least  $k_b T (\ln 2 + p \ln p + (1-p) \ln(1-p))$  amount of work is required to be done on the system [2]. It is important to note that the bound decays rapidly as  $p$  decreases from 1; with the bound being  $k_b T \ln 2$  for  $p = 1$  and zero for  $p = 0.5$ . In our study, we ensure that  $p > 0.95$  and assume that the erasure process is always successful.

The erasure protocol is described next where duty-ratio is the fraction of the time spent by the laser at the location,  $-L$  (see Fig. 4(c)), as compared to  $L$ ; higher the duty-ratio more is the time spent by the laser at  $-L$ . In the first phase of the protocol, the memory model of a Brownian particle in a symmetric double well potential is

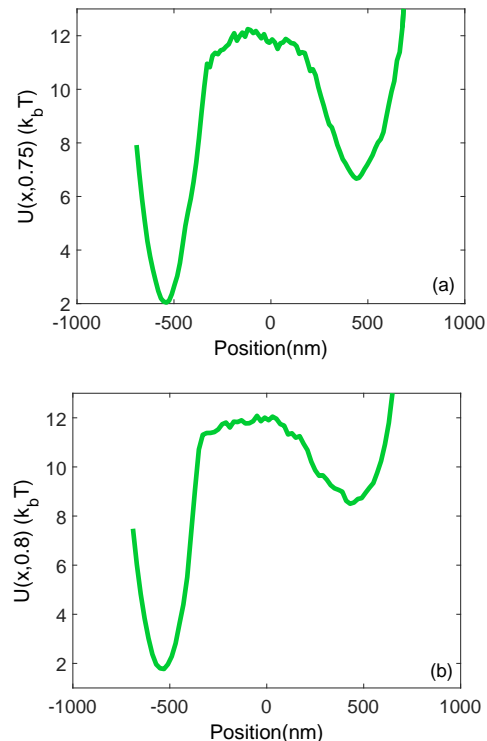


FIG. 3. Effect of duty-ratio on the nature of double well potential. Increasing the duty-ratio at  $-L$  from 0.75 to 0.8 increases the asymmetry of the potential.

obtained by maintaining a duty ratio of 0.5 for a duration of 10 seconds. Next, in the second phase of the protocol, an asymmetric well is realized, with the well at  $-L$  deeper than the well at  $L$ , which is obtained by maintaining the duty-ratio to be greater than 0.5 for a duration (dependent on the choice of  $d$ ) of  $\tau$  seconds. Finally, we revert the duty-ratio to a value of 0.5 to complete the ‘reset to zero’ process (for a duration of 10 seconds). The success of erasing the memory depends, on the magnitude of the deviation of the duty ratio from 0.5 and the time duration  $\tau$  during the second phase.

In the second phase, over the time duration  $\tau$ , the laser spends more time focused at  $-L$  than at  $L$ , enabling an asymmetric potential landscape as is observed in Fig. 3. Increasing the duty-ratio results in a lower barrier height for the right to left transition than for the left to right transition. It thus favors the transport of the bead from the right to the left well, if the bead is initially in the right well as shown in Fig. 4(a) and retains the bead in the left well if it was initially in the left well as shown in Fig. 4(b). The duration  $\tau$  is chosen to be a few multiples of the average exit time of the bead from the right well but less than the average exit time of the bead from the left well, which ensures a high likelihood of the bead’s final location to be in the left well. For example, we choose  $\tau$  as 30 seconds for the duty ratio of 0.7, which is approximately three times the observed exit time of the bead from the right well.

The above mentioned erasure mechanism ensures high

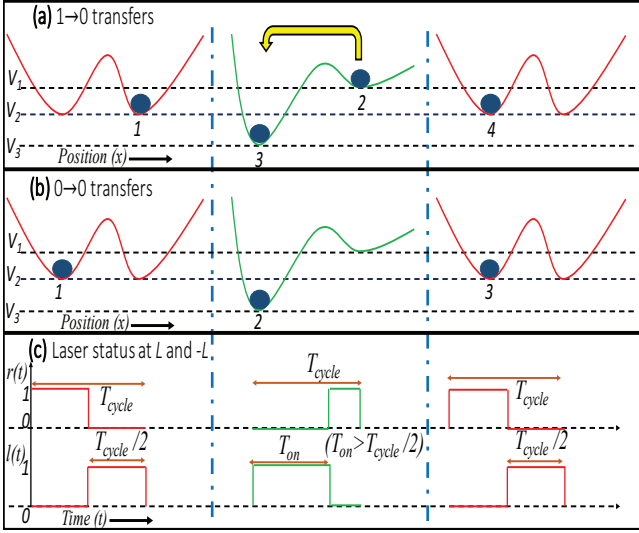


FIG. 4. (a) Schematic showing erasure process, with bead initially in the right well. The initial bead position is 1 (right well), with potential energy  $V_2$ . The duty-ratio  $d$  at left well is then increased, which lifts the bead and takes it to position 2 with energy  $V_1$ . Thermal fluctuations enables the bead to cross the barrier and reach position 3, with energy  $V_3$ . Decreasing the duty-ratio back to 0.5 lifts the bead to position 4, which has energy  $V_2$ . The process  $1 \rightarrow 2 \rightarrow 3 \rightarrow 4$  is the erasure process. (b) Schematic showing erasure process, with bead initially in the left well. Here, the process  $1 \rightarrow 2 \rightarrow 3$  is the erasure process. (c) The signals  $r(t)$  and  $l(t)$  denote the presence/absence status of the laser at  $L$  and  $-L$  respectively. A value of 1 means present and 0 means absent. To ensure a duty-ratio greater than 0.5, we maintain  $d = T_{\text{on}}/T_{\text{cycle}} > 0.5$ .

success proportion as reported in Fig. 5. It is seen that the duty-ratio of 0.65 yields success proportion significantly less than 0.95, while a duty-ratio  $> 0.7$  shows a success proportion greater than 0.95. Similar trends are reflected from Monte Carlo simulations as well as experiments as seen in Fig. 5. Thus, to ensure a high success proportion in order to demonstrate erasures with energy expenditure close to the Landauer's bound, we operate our erasure protocol at a duty ratio of at least 0.7. In the next section, we quantify the work done on the bead in an erasure process for a given duty-ratio.

### III. Erasure Thermodynamics

We now utilize the stochastic-energetics framework for Langevin systems [14, 15] and quantify the work done on the system, associated with erasure process realized by manipulation of duty-ratios. The external system does work on the bead by changing the duty-ratio, which results in modifying the potential felt by the bead. For an erasure process, the work done on the bead,  $dW$ , is given by,

$$dW = \sum_j [U(x(t_j), d(t_j^+)) - U(x(t_j), d(t_j^-))], \quad (5)$$

where  $d$  denotes the discontinuous parameter (here, the duty-ratio) changed by the external system, and  $t_j$  denotes the time instances when the parameter was changed

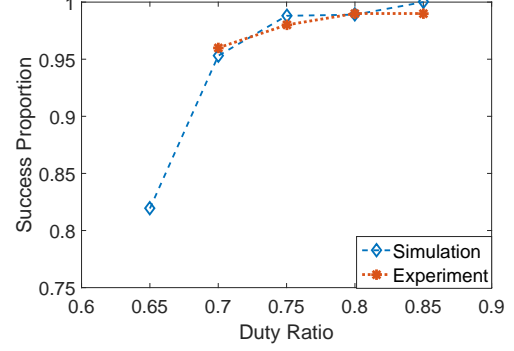


FIG. 5. Effect of duty-ratio on success proportion  $p$ . Duty-ratio of 0.65 has a success proportion of 0.82, whereas, duty-ratio greater than 0.7 yields success proportion higher than 0.95.

( $t_j^-$  and  $t_j^+$  denote the instants just before and after changing the parameter respectively).

Landauer's bound can be reached when the erasure process is performed in a quasi static manner. For an erasure performed over a large but finite duration  $\tau$ , the average work done on the system is [13],

$$\langle dW \rangle = dW_{\text{Landauer}} + \frac{B}{\tau} \quad (6)$$

where,  $dW_{\text{Landauer}} = k_b T \ln 2 = 0.693 k_b T$ . The duration for which an asymmetric double well potential is realized,  $\tau$ , is chosen to be a multiple of the exit time,  $\tau_e$ , of the bead from the right well. It is known that  $\tau_e \propto \frac{\exp(\delta U_r)}{\sqrt{k_r}}$ , [21] where  $\delta U_r$  is the barrier height of the right well,  $k_r$  is the stiffness of the right well and  $\exp(\cdot)$  is the exponential function. Note that  $d - 0.5$  is indicative of the asymmetric nature of the double well potential; higher the value, more the asymmetry. We determine the dependency of  $\delta U_r$  and  $k_r$  on  $\frac{1}{d-0.5}$  empirically. The dependency of normalized  $\delta U_r$  and  $k_r$  on  $\frac{1}{d-0.5}$  is shown in Fig. 6 and 7 respectively. It follows that  $\tau \propto \tau_e \propto \frac{\exp(\frac{0.99}{d-0.5})}{\sqrt{\frac{1}{d-0.5}}}$ . Substituting it in (6) for  $\tau$  leads to,

$$\langle dW \rangle = dW_{\text{Landauer}} + B \frac{\exp(-\frac{0.99}{d-0.5})}{\sqrt{d-0.5}}. \quad (7)$$

Reducing  $d$ , the time duration  $\tau$  required for successful erasures increases, whereby the erasure process approaches a quasi-static process. Thus, the duty-ratio provides a handle to realize quasi-static erasure processes using time multiplexed potentials.

The average work done on the bead  $\langle dW \rangle$ , for duty-ratio  $d > 0.7$  obtained using simulations and experiments is shown in Fig. 8 and Fig. 9 respectively. For a duty-ratio of 0.7, average work done on the system obtained from Monte Carlo simulations is  $0.73 \pm 0.037 k_b T$ , while experimentally for duty-ratio of 0.7, the average work done on the bead is obtained to be  $0.9 \pm 0.106 k_b T$ . The average work of  $0.9 \pm 0.106 k_b T$  to erase a bit of information is the closest to the Landauer's bound of  $k_b T \ln 2$



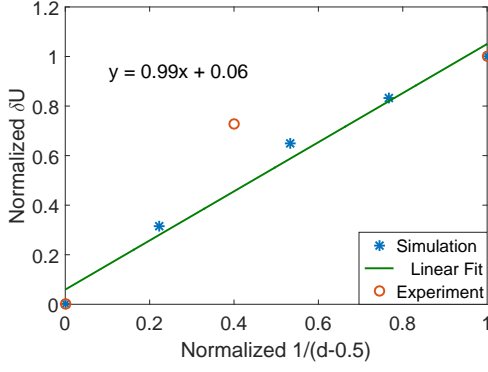


FIG. 6. The blue and red points represent normalized barrier height of right well as a function of  $\frac{1}{d-0.5}$  obtained using simulations and experiments respectively. The green line is the least squares fit to the simulation data points.

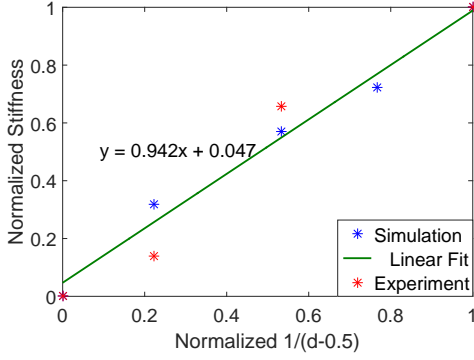


FIG. 7. The blue and red points represent normalized stiffness of right well as a function of  $\frac{1}{d-0.5}$  obtained using simulations and experiments respectively. The green line is the least squares fit to the simulation data points.

reported. As the duty-ratio is reduced ( $1/(d-0.5)$  increased), the average work done on the bead decreases, as observed in simulations as well as experiments.

We fit the model derived in (7),  $\langle dW \rangle_{fit} = A + B \frac{\exp(-\frac{0.99}{d-0.5})}{\sqrt{d-0.5}}$  to the average work done on the bead obtained by simulations and experiments for various duty-ratio values, with  $A$  and  $B$  being free parameters (see Fig. 9). Using simulation data we obtain  $A = 0.65k_bT$ ,  $B = 8.49k_bT$ , whereas for experimental data we have  $A = 0.70k_bT$ ,  $B = 35.04k_bT$ . It is seen that  $A$  (which represents the average work done on the system in the quasi-static case) has a value close to the Landauer bound of  $k_bT \ln 2 (= 0.693k_bT)$ , in both simulations as well as experiments.

The distribution of work done while erasing a bit at a duty-ratio of 0.7, obtained from simulations and experiments is shown in Fig. 10. It is evident that for a fraction of trajectories, the work done on the bead is less than the Landauer's bound; indeed, for some trajectories it is negative. However, the mean of the distribution is close to the Landauer's bound. Moreover, a bimodal nature of the distribution is evident. The mode on the

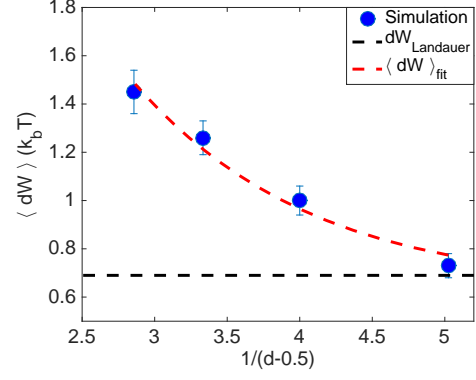


FIG. 8. The blue circles represent the average work done on the bead obtained using 300 Monte Carlo realizations (150,  $0 \rightarrow 0$  and 150,  $1 \rightarrow 0$  transfers) for duty ratio of 0.7, 0.75, 0.8, 0.85. The vertical lines represent the standard error in mean for each duty ratio. The black dotted line denotes the the Landauer bound of  $k_bT \ln 2$ . The red dotted line is the fit with the free parameters  $A$  and  $B$ .

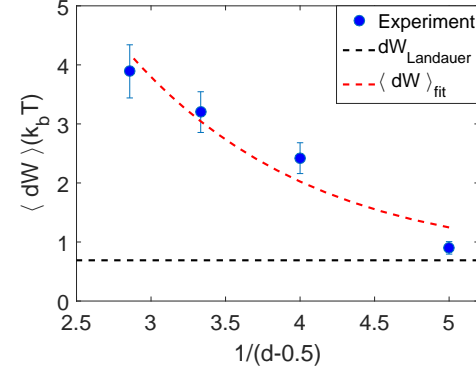


FIG. 9. The blue circles represent the average work done on the bead obtained from 100 experiments (50,  $0 \rightarrow 1$  and 50,  $1 \rightarrow 1$  transfers) for duty-ratio of 0.7, 0.75, 0.8, 0.85. The vertical lines represent the standard error in mean for each duty-ratio. The black dotted line denotes the the Landauer bound of  $k_bT \ln 2$ . The red dotted line is the fit with the free parameters  $A$  and  $B$ .

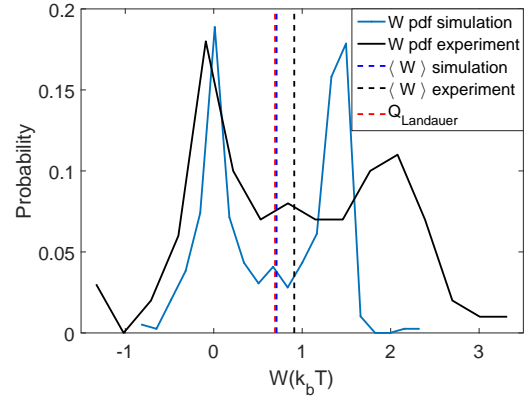


FIG. 10. Distribution of work done on the bead obtained from simulations and experiments for a duty-ratio of 0.7. The nature of the distribution is bimodal.

right in Fig. 10 corresponds to work done on the particle for transition from right to left well (or  $1 \rightarrow 0$ ) and mode on the left corresponds to transition from left to left well (or  $0 \rightarrow 0$ ). The characteristics of the simulation data are confirmed by experiments as shown in Fig. 10. On increasing the duty-ratio, the mode on the right shifts further to the right as work done on the bead is higher for higher duty-ratios. This results in an increase in the standard error in mean on increasing duty ratio as shown by the length of the blue bars in Fig. 8 and Fig. 9.

Thus we have demonstrated that a single bit memory and its associated erasure protocol can be realized by multiplexing a laser between two locations. The resulting energetics can be effectively accounted for in the framework developed by Sekimoto and the magnitude of the deviation of the duty-ratio of multiplexing from 0.5 provides an effective means for driving the erasure process toward a quasistatic process.

**Error Quantification:** The primary sources of error in the average work done on the system computed from position measurements are introduced by the photodiode based measurements. The error statistics of the photodiode used in the experiments are quantified in [22] and is shown to have zero mean and a standard deviation of the order of a nanometer. Assuming that error in position measurement  $e_x$  is independent of the actual bead position  $x$ , the average error in potential energy of the bead  $e_U$  is given by,

$$\begin{aligned}\langle e_U \rangle &= \left\langle \frac{1}{2}k(x + e_x - L)^2 - \frac{1}{2}k(x - L)^2 \right\rangle \\ &= \frac{1}{2}k\langle e_x^2 \rangle \sim 10^{-3}k_bT.\end{aligned}$$

Thus, error in obtaining the work done on the bead in a realization of erasure is of the order of  $10^{-3}k_bT$ .

#### IV. Conclusions

In this article, we study the thermodynamics of a Brownian particle influenced by the time multiplexing of a single harmonic potential of finite width. A Monte Carlo simulation framework for a Brownian particle under the influence of a time multiplexed laser is also developed and shown to obey qualitative trends observed in experiments. We demonstrate that the duty-ratio provides a handle on the speed of the erasure process and its approach to reversibility. It is established through experiments and simulations that reducing duty ratio results in erasure process with average work done approaching  $k_bT \ln 2$ ; which is the minimum average work required to erase one bit of information. Furthermore, the method is easy to implement on a standard optical tweezer setup. The insights obtained from this article can be potentially leveraged to realize practical devices that yield erasure mechanisms with energetics in the order of  $k_bT \ln 2$ .

**Acknowledgement:** We would like to thank Prof. Arun Majumdar, Stanford University for initial discussion about the problem, Prof. Srinivasa Salapaka, University of Illinois, Urbana Champaign for his comments, Tanuj Aggarwal, Cymer LLC and Subhrajit Roychowdhury, GE Research for their contribution towards building the optical tweezer setup. The research reported is supported by National Science Foundation under the grant CMMI-1462862.

**Author Contributions:** S.T. and S.B contributed equally to this work. S.T., S.B. and M.S. conceptualized the work. S.T. and S.B. developed the computational framework and conducted experiments.

- 
- [1] R. Landauer, IBM Journal of Research and Development **5**, 183 (1961).
  - [2] J. M. Parrondo, J. M. Horowitz, and T. Sagawa, Nature Physics **11**, 131 (2015).
  - [3] K. Shizume, Physical Review E **52**, 3495 (1995).
  - [4] R. Dillenschneider and E. Lutz, Physical Review Letters **102**, 210601 (2009).
  - [5] B. Lambson, D. Carlton, and J. Bokor, Physical Review Letters **107**, 010604 (2011).
  - [6] B. Piechocinska, Physical Review A **61**, 062314 (2000).
  - [7] T. Sagawa and M. Ueda, Physical Review Letters **102**, 250602 (2009).
  - [8] A. Bérut, A. Arakelyan, A. Petrosyan, S. Ciliberto, R. Dillenschneider, and E. Lutz, Nature **483**, 187 (2012).
  - [9] Y. Jun, M. Gavrilov, and J. Bechhoefer, Physical Review Letters **113**, 190601 (2014).
  - [10] M. Gavrilov and J. Bechhoefer, Physical Review Letters **117**, 200601 (2016).
  - [11] J. Hong, B. Lambson, S. Dhuey, and J. Bokor, Science Advances **2**, e1501492 (2016).
  - [12] K. Sekimoto, Journal of the Physical Society of Japan **66**, 1234 (1997).
  - [13] K. Sekimoto and S. Sasa, Journal of the Physical Society of Japan **66**, 3326 (1997).
  - [14] K. Sekimoto, Progress of Theoretical Physics Supplement **130**, 17 (1998).
  - [15] K. Sekimoto, *Stochastic energetics*, Vol. 799 (Springer, 2010).
  - [16] A. Ashkin, J. Dziedzic, J. Bjorkholm, and S. Chu, Optics letters **11**, 288 (1986).
  - [17] K. Visscher and S. M. Block, Methods in Enzymology **298**, 460 (1998).
  - [18] K. C. Neuman and S. M. Block, Review of scientific instruments **75**, 2787 (2004).
  - [19] S. Bhaban, S. Talukdar, and M. Salapaka, in *2016 American Control Conference (ACC)* (IEEE, 2016) pp. 5823–5829.
  - [20] C. H. Bennett, International Journal of Theoretical Physics **21**, 905 (1982).
  - [21] C. W. Gardiner *et al.*, *Handbook of stochastic methods*, Vol. 4 (Springer Berlin, 1985).
  - [22] T. Aggarwal and M. Salapaka, Review of Scientific Instruments **81**, 123105 (2010).